Journal Pre-proof

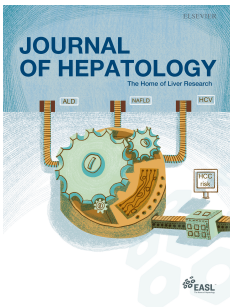

A structurally engineered fatty acid, icosabutate, suppresses liver inflammation and fibrosis in NASH

David A. Fraser, Xiaoyu Wang, Jenny Lund, Nataša Nikolić, Marta Iruarrizaga-Lejarreta, Tore Skjaeret, Cristina Alonso, John J.P. Kastelein, Arild C. Rustan, Yong Ook Kim, Detlef Schuppan

PII: S0168-8278(21)02244-3

DOI: https://doi.org/10.1016/j.jhep.2021.12.004

Reference: JHEPAT 8532

To appear in: *Journal of Hepatology*

Received Date: 7 January 2021

Revised Date: 1 December 2021

Accepted Date: 2 December 2021

Please cite this article as: Fraser DA, Wang X, Lund J, Nikolić N, Iruarrizaga-Lejarreta M, Skjaeret T, Alonso C, Kastelein JJP, Rustan AC, Kim YO, Schuppan D, A structurally engineered fatty acid, icosabutate, suppresses liver inflammation and fibrosis in NASH, *Journal of Hepatology* (2022), doi: https://doi.org/10.1016/j.jhep.2021.12.004.

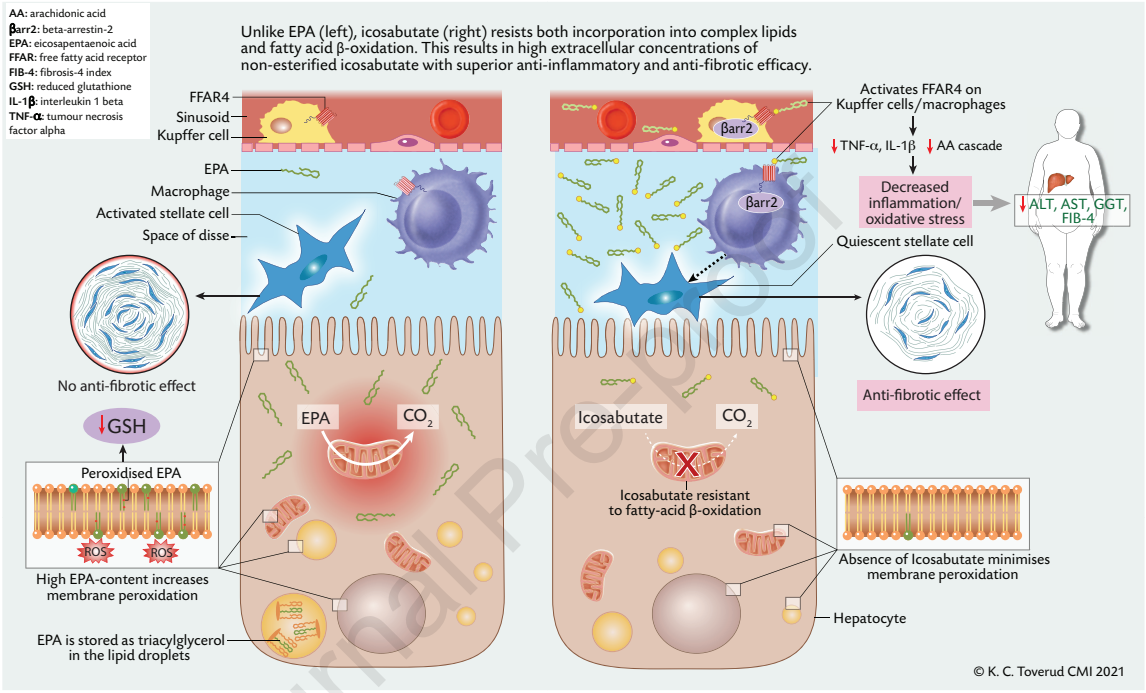

A structurally engineered fatty acid, icosabutate, suppresses liver inflammation and fibrosis in NASH

David A Fraser[1#], Xiaoyu Wang[2,3#], Jenny Lund[4], Nataša Nikolić[4], Marta Iruarrizaga-Lejarreta[5], Tore Skjaeret[1], Cristina Alonso[5], John J.P. Kastelein[6], Arild C. Rustan[4], Yong Ook Kim[2], Detlef Schuppan[2,7]*

1 NorthSea Therapeutics, Amsterdam, The Netherlands; 2 Institute of Translational Immunology and Research Center for Immune Therapy, University Medical Center, Mainz, Germany; 3 Institute of Biochemistry and Molecular Biology, College of Life Science and Health, Northeastern University, Shenyang, China; 4 Section for Pharmacology and Pharmaceutical Biosciences, Department of Pharmacy, University of Oslo, Norway; 5 OWL Metabolomics, Parque Tecnológico de Bizkaia, Derio, Spain; 6 Department of Vascular Medicine, Academic Medical Center, University of Amsterdam, Amsterdam, The Netherlands, 7 Division of Gastroenterology, Beth Israel Deaconess Medical Center, Boston, MA, USA. #These authors contributed equally to this work

*****To whom correspondence should be addressed:
Institute of Translational Immunology and Research Center for Immune Therapy
University Medical Center, Mainz, Germany
Phone: + 49 6131 17 7356
Fax: + 49 6131 17 7356
Email: detlef.schuppan@unimedizin-mainz.de

Electronic word count (6468)

Running title: Icosabutate for the treatment of NASH

Keywords: ALT, antifibrotic, collagen, FIB-4, icosabutate, omega-3 fatty acid, oxidative stress, glutathione, steatohepatitis

List of abbreviations

AA, arachidonic acid; ALT, alanine aminotransferase; AST, aspartate transaminase; CD, choline deficient; CE, cholesteryl ester; CS, choline sufficient; Col1A1, type 1 collagen alpha 1; cPLA2, cytosolic phospholipase 2; DAG, diacylglycerol; EPA, eicosapentaenoic acid; EXE, exenatide extended-release; FIB-4, Fibrosis-4 index; FFA, free fatty acid; FFAR, free fatty acid receptor; GSH, glutathione; GSSG, glutathione disulfide; H&E, haematoxylin and eosin; HETE, hydroxyeicosatetraenoic acid; HODE, hydroxyoctadecadienoic acid; HYP, hydroxyproline; ICOSA-L, low-dose icosabutate; ICOSA-H, high-dose icosabutate; IL , interleukin; LA, linoleic acid; LCn-3FA, long-chain omega-3 fatty acid; PC, phosphatidylcholine; PDGF, platelet derived growth factor; PL, phospholipid; PUFA, polyunsaturated fatty acid; SMA, smooth-muscle actin; SR, Sirius Red; TAG, triacylglycerol; TGFβ, transforming growth factor beta; TIMP1, tissue inhibitor of metalloproteinase 1; TNFα, tumor necrosis factor alpha; TriHOME, trihydroxyoctadecenoic acid; UHPLC-MS, ultra-high performance liquid chromatography mass spectrometry

Funding

DS receives project-related support from the German Research Foundation (DFG) Collaborative Research Center (CRC) grants SFB 1066 project B3 and CRC 1292 project B10, and by EU Horizon 2020 projects under grant agreements nr. 634413 (EPoS, European Project on Steatohepatitis) and nr. 777377 (LITMUS, Liver Investigation on Marker Utility in Steatohepatitis).

Author Contributions

DF and DS equally designed and supervised the study, wrote and edited the manuscript. XYW performed the *in vivo* experiments, contributed to experimental design and evaluation of the experimental results. TS was responsible for the chemical synthesis and quality control of icosabutate. JL, NN and ACR performed and analysed the *in vitro* cell culture assays. MIL and CA performed and analysed the liver lipidomics. JK was lead investigator of the clinical study and

central in its evaluation. YOK designed and performed several experiments. All authors helped writing and editing the manuscript.

Conflict of Interest

NorthSea Therapeutics BV acquired the commercial rights for icosabutate. DS and JK are paid consultants and have stock options in NorthSea Therapeutics. DF and TS are employees of NorthSea Therapeutics BV but had no role in data collection. All other authors declare that the research was conducted in the absence of any commercial or financial relationships that could be construed as a potential conflict of interest.

Data availability

All the data used to support the findings of this study are included within the article. Reagents and resources are included in the Methods or Supplementary Materials.

Lay summary

Long-chain omega-3 fatty acids can potentially target multiple pathways regulating hepatic inflammation and fibrosis. However, their susceptibility to peroxidation and use as an energy source may limit their clinical efficacy. Here we show that a structurally modified omega-3 fatty acid, icosabutate, is minimally incorporated into hepatocytes and resists utilisation as an energy source. This results in a high extracellular concentration and allows icosabutate to avoid the worsening of hepatic oxidative stress seen in response to an unmodified omega-3 fatty acid. The structural changes also markedly improve anti-inflammatory and anti-fibrotic efficacy in a mouse model of non-alcoholic steatohepatitis (NASH). A hepatoprotective effect of icosabutate in patients with elevated circulating lipids at increased risk of NASH is also shown, where rapid reductions in markers of liver injury are observed.

Abstract

Background and Aims: Although long-chain omega-3 fatty acids (LCn-3FAs) regulate inflammatory pathways of relevance to non-alcoholic steatohepatitis (NASH), their susceptibility to peroxidation may limit their therapeutic potential. We compared the metabolism of eicosapentaenoic acid (EPA) with an engineered EPA derivative (icosabutate) in human hepatocytes *in vitro* and their effects on hepatic glutathione metabolism, oxidised lipids, inflammation, and fibrosis in a dietary mouse model of NASH, and in patients prone to fatty liver disease.

Methods: Oxidation rates and cellular partitioning of EPA and icosabutate were compared in primary human hepatocytes. Comparative effects of delayed treatment with either low- (56 mg/kg) or high-dose (112 mg/kg) icosabutate were compared with EPA (91 mg/kg) or a glucagon-like peptide 1 receptor agonist in a choline deficient (CD), L-amino acid defined NASH mouse model. To assess potential clinical translation, effects on elevated liver enzymes and FIB-4 were assessed in overweight, hyperlipidemic subjects with an increased risk of NASH.

Results: In contrast to EPA, icosabutate resisted oxidation and incorporation into hepatocytes. Icosabutate also reduced inflammation and fibrosis in conjunction with a reversal of CD-diet induced changes in the hepatic lipidome. EPA had minimal effect on any parameter and even worsened fibrosis in association with depletion of hepatic glutathione. In dyslipidemic subjects at risk of NASH, icosabutate rapidly normalised elevated plasma ALT, GGT and AST and reduced FIB-4 in subjects with elevated ALT and/or AST.

Conclusion: Icosabutate avoids hepatocyte accumulation and confers beneficial effects on hepatic oxidative stress, inflammation and fibrosis in mice. In conjunction with reductions in markers of liver injury in hyperlipidemic subjects, the findings suggest that structural engineering of LCn-3FAs offers a novel approach to the treatment of NASH.

Introduction

The pathogenesis of non-alcoholic steatohepatitis (NASH) is complex, with multiple pathways driving inflammation, hepatocyte damage and fibrosis (1-3). The ability of long-chain omega-3 fatty acids (LCn-3FAs), e.g., eicosapentaenoic acid (EPA), to inhibit platelet activation (4), target nuclear (5) and extracellular (6) receptors and favourably alter the balance of NASH-associated oxylipins (oxygenated fatty-acid metabolites) (7, 8), fulfils the need for pleiotropic targeting of the disease. However, 12 months treatment with EPA ethyl ester (1.8 or 2.7 g/day) had no effect on liver histology in patients with NASH (9).

Given the importance of oxidative stress as a driver of NASH (10), a potential liability countering the beneficial effects of LCn-3FAs for the treatment of NASH is their susceptibility to peroxidation due to the high number of allylic double bonds (11). Increased oxidative stress in response to high-dose LCn-3FAs occurs in humans (12-14) and in rodent models of both NASH and alcoholic steatohepatitis (ASH) (15, 16).

Avoidance of incorporation into complex lipids, in particular cell membranes (17), could limit the LCn-3FA associated increase in oxidative stress. Icosabutate is a structurally engineered EPA derivative currently being evaluated in a phase 2b clinical study for the treatment of NASH (NCT04052516). In contrast to naturally occurring LCFAs that are transported in chylomicrons from the gut to the periphery (18), icosabutate directly targets the liver via the portal vein and has demonstrated promising results in rodent NASH models (19, 20).

We have compared the cellular metabolism of icosabutate versus unmodified EPA in primary human hepatocytes *in vitro*. We also compared their effects upon hepatic lipidomics, glutathione metabolism, inflammation, fibrosis, and glucose tolerance in an optimized dietary, non-transgenic, fibrosing choline-deficient L-amino acid defined (CD) moderate fat diet mouse model (21, 22) using the GLP-1R agonist, exenatide extended-release (EXE) as a positive control. To further assess the potential translatability of the rodent findings to humans, we assessed time-course changes in elevated plasma alanine aminotransferase (ALT), aspartate transaminase (AST) and gamma-glutamyltransferase (GGT) levels in subjects with increased risk of NASH and cardiovascular disease (CVD) treated for up to 12 weeks with oral icosabutate (600

mg q.d.) or placebo (23-25). Fibrosis-4 (FIB-4) scores were also measured in subjects with elevated baseline ALT and/or AST.

Methods

For detailed methods refer to the Supplement

Cell experiments

Primary human hepatocytes grown in 12- or 96-well plates were incubated with 5 µM or 25 µM (0.2 and 0.5 µCi/ml, respectively) ^{14}C-Icosabutate or ^{14}C-EPA for 24 h. To assess lipid distribution, cells were washed with PBS, harvested in 250 µl 0.1% SDS and cellular lipids extracted and separated as described earlier (26), followed by liquid scintillation counting. Cellular and extracellular lipids were calculated in relation to total cell protein content measured according to Pierce BCA Protein Assay Kit. To measure fatty acid oxidation, cells were incubated for 24 h before CO_2 was trapped for another 4 h. The CO_2 produced was captured by filters soaked with sodium hydroxide (27). Cellular ^{14}C-CO_2 production by was related to total cell protein content measured according to Bradford (28).

Choline-deficient (CD) diet NASH mouse model

Ninety male C56BL/6J mice (9 weeks old) were divided into 2 experimental groups (45 mice per group) and fed either a choline-sufficient (CS, n = 45) or choline-deficient (CD, n = 45) L-amino acid defined high sucrose, moderate fat (containing 31 % of calories from fat) diet, plus 0.2% cholesterol for 12 weeks (**Table S1**). From week 7-12 groups of 9 received either no treatment (CD, CS), 0.15mmol/kg icosabutate (ICOSA-L), 0.3 mmol/kg icosabutate (ICOSA-H), 0.3 mmol/kg EPA in chow, or exenatide extended-release (EXE) at 0.4 mg/kg once-weekly injected subcutaneously (EXE dosage utilised in earlier studies (29)). Animals were sacrificed after 12 weeks.

Intraperitoneal glucose tolerance test (IPGTT) was performed at study end as described previously (30). **Liver hydroxyproline** was quantified from 150 mg of frozen liver (31), to determine liver collagen content.

Staining of liver sections

Liver cryosections were stained for lipid with Direct Red 80, Sudan III, or Oil red O; collagen and CD68 were stained on formalin fixed sections (22, 30, 32). In each animal, stained areas were

quantitated using ImageJ software, and cells were counted in a minimum of 10 randomly selected fields (30, 32, 33).

RT-qPCR analysis

TaqMan probes and primers are summarized in **Table S2**. RNA levels were normalised to Gapdh using the relative standard curve method (22, 30-33).

Hepatic lipidomic analysis was performed with LC-MS/MS as described (19).

Human study samples

Subjects with abnormal baseline ALT, GGT or AST were identified from 3 previously published placebo controlled, randomized clinical trials (NCT02364635, NCT01893515 and NCT01972178) of icosabutate treatment (600 mg q.d.) versus placebo in overweight/obese hyperlipidemic subjects at high risk of NASH and cardiovascular disease (23-25). Liver enzymes were assessed over 5 time points from baseline to study end (4 and 12 weeks). FIB-4 scores were calculated [age (years) × AST (U/L)/[platelets (10^9/L) × $ALT^{1/2}$ (U/L)] in subjects with elevated baseline ALT and/or AST (34).
Further detailed information for experiments performed *in vivo* and *in vitro* are detailed in Supplemental Methods.

Statistical Analysis Data from the mouse model and human subjects were evaluated using one-way ANOVA (two-way ANOVA for IPGTT) with multiple comparison *post-hoc* analysis except for FIB-4 scores where Wilcoxon paired signed rank test was used. For cellular lipids and hepatic lipidomics, differences between groups were tested using an unpaired t-test. Data are presented as mean values ± SEM (standard error of mean) with significance set at α = 5% for all comparisons. All statistical data was produced using GraphPad Prism 8.2.1 (GraphPad software, La Jolla, USA) except hepatic lipidomics (MassLynx 4.1 software) in which all calculations were performed using statistical software package R v.3.1.1 (R Development Core Team, 2011; https://cran.r-project.org/).

Results

Icosabutate is minimally incorporated into complex lipids and is resistant to use as a cellular energy source

Icosabutate is structurally designed to (A) avoid incorporation into complex lipids via an ethyl-group in the α-position and (B) resist β-oxidation via incorporation of an oxygen atom into the β-position (**Fig.1A**). As is shown in **Table 1**, in contrast to EPA, minimal amounts of icosabutate/icosabutate metabolites are found as complex lipids after 24 h incubation of primary human hepatocytes (15 to 19-fold lower concentrations in total intracellular lipids than EPA). Accordingly, higher concentrations of icosabutate were found in the extracellular fraction (9- and 14-fold higher than the intracellular pool at 5 and 25 μM, respectively) (**Fig.1B)**. Conversely, EPA concentration was 6.5- and 4-fold higher in the intracellular versus the extracellular pool at the corresponding concentrations. Minimal increases in CO_2 production from primary human hepatocytes incubated with icosabutate demonstrate the efficacy of the oxygen substitution in the β-position (**Fig.1C**), effectively preventing its own metabolism via fatty acid β-oxidation. Overall, these results demonstrate how specific structural modifications to EPA minimise both fatty acid β-oxidation and esterification into complex lipids in human hepatocytes, resulting in a high extracellular concentration.

A GLP-1R agonist (EXE) induces pronounced effects on body weight, food intake, liver weight, plasma ALT and glycemic control in mice with diet-induced NASH

As expected, and in part due to its anorexigenic effect (35), EXE significantly improved multiple parameters related to obesity and NASH. Thus, EXE reduced body weight by 22% (**Fig.2A**) in association with a decreased calculated food intake (-29%) versus the untreated CD-diet-fed mice (**Fig.2B**), while neither icosabutate nor EPA affected body weight or calculated food intake. The CD-diet (which attenuates hepatic export of TAG via inhibition of phosphatidylcholine synthesis) induced an increase in liver weight relative to the choline-sufficient (CS) control diet (**Fig.2C**). In mice fed the CD-diet, EXE markedly reduced liver weight as compared to the CD-diet alone, whereas icosabutate and EPA had no effect (**Fig.2C**). The CD-diet induced an increase in plasma ALT (**Fig.2D**) that was reduced by treatment with ICOSA-H and EXE treatment, whereas

no changes were observed in plasma AST (**Fig.2E**). EXE markedly improved glucose tolerance, as measured by the intraperitoneal glucose tolerance test (**Fig.2F**) in CS-diet-fed mice. ICOSA-L and ICOSA-H modestly improved glucose tolerance, whereas EPA was without effect. CS-diet-fed mice displayed a more pronounced glucose excursion versus CD-diet-fed mice (**Fig.S2**).

Late onset treatment with icosabutate and EXE, but not EPA, decreases hepatic fibrosis and inflammation

Representative images from all treatment groups are shown in **Fig.3A**. The CD-diet markedly increased hepatic fibrosis, as evidenced by a 2.2-, 3.5 and 2.8-fold increase in collagen deposition measured via relative (mg per g liver) and total (per liver) hydroxyproline (HYP) content, and Sirius Red (SR) morphometry, respectively (**Fig.3B-D**). Icosabutate was the only treatment that significantly reduced all three quantitative measures of fibrosis. Notably, despite 6 weeks of the CD-diet before treatment initiation, ICOSA-L reduced fibrosis (SR) by 69% versus no treatment to a level comparable with the control CS mice that developed no detectable fibrosis (**Fig.3D**). ICOSA-H and EXE also significantly decreased fibrosis (SR) versus untreated CD mice by 37% and 41%, respectively. EXE reduced total **(Fig.3B**), but not relative HYP content in association with the markedly reduced liver weight in EXE-fed mice. EPA had no significant effect on HYP content and significantly increased collagen proportionate area (**Fig.3D**).

Effects of delayed treatment with icosabutate upon hepatic macrophage content and expression of hepatic inflammation and fibrosis related genes

Representative images of CD68 and YM1+ stained livers from CD treatment groups are shown in **Fig.4A.** Icosabutate or EXE did not affect total macrophage numbers (CD68+) (**Fig.4B**). Icosabutate, but not EXE, induced a dose-dependent decrease in YM1+ M2-type macrophages (**Fig.4C)**. The CD-diet upregulated all measured hepatic inflammation and fibrosis related genes versus the CS-diet (**Fig.5A-I**). Icosabutate at both doses significantly attenuated the CD-diet induced increases in all genes except for *acta2* (αSMA) (**Fig. 5E**) and *tgfb1* (**Fig.5F**) at the low-dose. EXE also showed significant inhibitory effects but did not alter transcripts encoding PDGFRβ, PDGF-B and TGFβ1 (**Fig.5B,C,F**). EPA only reduced *timp1*, *acta2* and IL-1β (**Fig.5D,E,H**) expression.

EPA exacerbates the CD-diet induced decrease in hepatic glutathione

Glutathione plays a pivotal role in cellular protection from lipid peroxidation (36). Given the pronounced cellular accumulation of EPA versus icosabutate in hepatocytes and the susceptibility of EPA to peroxidation, we compared their effects on hepatic reduced (GSH) and oxidised (GSSG) glutathione as markers of cellular redox status. The CD-diet induced a 38% decrease in hepatic GSH compared to the CS-diet, which was further exacerbated by EPA-treatment (37% lower than CD-diet mice) (**Fig.6A**). GSSG levels were maintained in response to the CD-diet but were significantly reduced by ICOSA-H (**Fig.6B**). Secondary to the decrease in GSH, the CD-diet significantly decreased the GSH/GSSG ratio, an effect that was offset by treatment with ICOSA-H (**Fig.6C**). In contrast, EPA worsened the GSH/GSSG ratio in the CD-diet mice, driven by the decrease in GSH. Peroxidation of EPA prior to ingestion could be ruled out, since the GSH/GSSG ratio in the CS-diet fed groups was unchanged by EPA treatment (**Fig.6D**). Overall, these data suggest that the CD-diet associated depletion of hepatic GSH is exacerbated by EPA, whereas ICOSA-H improves cellular redox status.

Since EPA mediates its anti-inflammatory effects in part via replacement of arachidonic acid (AA) in cell membranes, we also measured hepatic stores of AA in phospholipids (PL; phosphatidylcholine species) and diacylglycerols (DAG). The CD-diet induced a significant 51% increase in hepatic DAG-AA (**Fig.6E**) and a 28% decrease in PL-AA (**Fig.6F**). Both doses of icosabutate and, to a lesser extent EPA, attenuated the CD-diet induced increase in DAG-AA, whereas concentrations of PL-AA were lower in icosabutate treated mice only (**Fig.6E,F**). To assess if the conversion of linoleic acid (LA) and AA to oxylipins was inhibited by either treatment, we also assessed the hepatic 13-hydroxyoctadecadienoic acid (HODE)/LA and (11-, 12- and 15-)hydroxyeicosatetraenoic acid (HETE)/AA ratios. Although there was no significant change in the CS- versus CD-diet groups, icosabutate (both doses) significantly reduced the 13-HODE/LA ratio (a ratio that in plasma is positively associated with NASH in humans (37)) (**Fig.6H**) and the HETE/AA ratio (ICOSA-H only). Despite lack of incorporation into phospholipid membranes, only icosabutate reduced hepatic concentrations of AA-derived (11(R)- and 15(S)-HETE) and LA-derived (13-HODE and 9,12,13-TriHOME) oxylipins (**Fig.6I-L**).

Overall, these data suggest that icosabutate reduces hepatic AA stores, the conversion of LA and AA to oxylipins and the concentrations of both AA and LA derived oxylipins.

Icosabutate prevents the CD-diet induced changes in hepatic lipids

As shown in **Fig.7**, the most significant changes in hepatic lipids induced by the CD-diet were increases in DAG, TAG, TriHOMEs (trihydroxy-octadecenoic acids) and cholesteryl esters (ChoE), all of which were significantly lowered by treatment with icosabutate versus CD-diet alone (except ChoE by low-dose icosabutate). The CD-diet also significantly increased omega-6 fatty acids, total poly- and monounsaturated fatty acids (PUFA/MUFAs) and glycine conjugated bile acids (GCBA). Apart from GCBA, icosabutate significantly prevented these increases. EPA had relatively minor effects on hepatic lipids but did prevent the CD-diet-induced increase in GCBA. The CD-diet significantly lowered oxoODEs (oxo-octadecadienoic acids), whereas this decrease was prevented by icosabutate. As expected from the changes in individual HETEs noted above, icosabutate, but not EPA, decreased the concentrations of NASH associated HETEs (8). Overall, except for GCBA, the hepatic lipidomic data suggest that icosabutate prevents CD-diet induced changes in hepatic lipids.

Icosabutate is a full FFAR4 (β-arrestin-2 pathway) agonist

As we found that icosabutate is predominantly found in the extracellular pool, we measured its activity towards free fatty acid receptor 4 (FFAR4). FFAR4 is a membrane bound receptor highly expressed on Kupffer cells/macrophages and activation via LCn-3FAs induces potent anti-inflammatory effects in rodents (6). Icosabutate fully activated FFAR4 via the β-arrestin-2 pathway at a concentration of 33 μM, with an EC50 of 15.5 μM **(Fig. S1)**. Interestingly this EC50 value is approximately 3-fold lower than the portal vein C_{max} of icosabutate in rats at a therapeutic dose (19).

Icosabutate rapidly decreases markers of liver injury in dyslipidemic subjects at high-risk of NASH/CVD.

To assess the potential translatability of the rodent findings to humans, we performed a post-hoc analysis of changes in elevated markers of liver inflammation (ALT, AST), glutathione metabolism (GGT) and fibrosis (FIB-4 score) (34) in subjects at high risk of NASH and CVD

(hyperlipidemic, overweight/obese) treated for up to 12 weeks with icosabutate (600 mg q.d.) or placebo (23-25). Subjects with abnormal baseline ALT (>40 U/L), GGT (>38 U/L females, >51 U/L males) or AST (>34 U/L) from 3 clinical trials with icosabutate were identified. The numbers of subjects identified with elevated baseline levels for icosabutate and placebo groups, respectively, were 16 and 19 (ALT), 33 and 35 (GGT), 11 and 13 (AST).

The baseline characteristics of the overall study population are shown in **Fig.8A**. Icosabutate treatment rapidly reduced plasma ALT, with significant reductions versus baseline seen at all time-points. Median ALT decreased by 49% (from 57 U/L to 29 U/L) from baseline to study end (**Fig.8B**) in response to icosabutate. Median AST (**Fig.8D**) was similarly decreased at all time points with icosabutate treatment (from 42 U/L at baseline to 28 U/L at study end). Rapid normalisation of elevated plasma GGT was also observed in response to icosabutate treatment, with significant decreases at all time-points (**Fig.8F**). Median GGT was decreased by 44% (from 62 U/L to 35 U/L) from baseline to study end. In contrast to icosabutate the placebo group demonstrated minimal changes in liver enzymes **(Fig.8C,E,G)**. FIB-4 scores were calculated at baseline and study end in all subjects with elevated ALT and/or AST at baseline (18 and 19 subjects in the icosabutate and placebo groups respectively). Icosabutate treatment significantly reduced FIB-4 scores, with 4/7 subjects in the previously classified (34) 'intermediate risk of developing severe liver disease' category moving into the 'low-risk' category **(Fig.8H).** No significant difference was observed in placebo treated subjects **(Fig.8I**).

Discussion

We have shown that, in direct contrast to EPA, icosabutate resists accumulation in primary human hepatocytes *in vitro* and avoids the EPA-associated worsening of hepatic glutathione depletion *in vivo*. The *in vitro* findings demonstrate that specific structural modifications to EPA, as exemplified by icosabutate, can profoundly alter its cellular partitioning and metabolism, resulting in a much higher enrichment in the extracellular relative to the intracellular pool. Importantly icosabutate, but not EPA, effectively reduced hepatic fibrosis and fibrogenesis in a CD-diet mouse model resembling human NASH. This was accompanied by a significant reduction in key inflammatory genes and hepatic concentrations of multiple NASH associated lipid species in mice and reductions in multiple markers of liver injury in subjects at risk of NASH.

Both doses of icosabutate significantly reduced liver collagen in mice as assessed by hydroxyproline content (both relative and total) and SR morphometry. The degree of reduction was surprising given that mice received the fibrosis-inducing CD-diet for 6 weeks before commencing treatment with icosabutate. Fibrosis has been reported to progresses continuously from week 4 up to week 24 in response to a CD-diet (22). However, as we do not have liver samples from mice immediately prior to treatment initiation after week 6 on the CD-diet, it is uncertain if, and how much, fibrosis was present at this stage. The difference in efficacy shown via the biochemical collagen quantification (hydroxyproline) and SR morphometry may be related to the former measuring tissue including portal tracts with dense collagen (underestimating the more delicate sinusoidal collagen), while the latter underestimates portal in favour of parenchymal collagen. The anti-fibrotic effect of icosabutate thus appears to be most prominent in the functionally relevant perisinusoidal area (38). Notably, EPA had no effect on fibrosis as measured by HYP content, with significant worsening in fibrosis as measured by SR morphometry. The lack of efficacy of EPA in the current model is in line with the lack of histological response to EPA supplementation (1.8 or 2.7 g/day) in patients with NASH (9).

The histological findings are in accordance with the decreases in hepatic levels of transcripts regulating fibrosis, fibrolysis and inflammation, where the most pronounced decreases occurred in response to icosabutate. Interestingly, high-dose icosabutate reduced M2-type macrophages, viewed typically as an anti-inflammatory phenotype. However, although not significant, the

relative reduction of CD68 (as a general macrophage marker) was comparable. We speculate that icosabutate reduces the influx of monocytes that would have differentiated into either M1- or M2-type macrophages. Moreover, as we previously showed (33), phenotypical M2 macrophages can have pro-inflammatory functions during liver disease progression, in contrast to beneficial functions once the disease trigger is removed. In contrast, EXE increased YM1 expressing M2-type macrophages that have been associated with worsening of fibrosis during progressive disease (2, 30, 32, 33, 39). However, the role of M2-type macrophages in fibrosis is complex, since there appears to exist a yet ill-defined M2-macrophage subset that suppresses both inflammation and fibrosis and that may speed up fibrosis resolution once the inflammatory stimulus has disappeared (2, 40). In this context, except for a reduction in key pro-inflammatory cytokines, there was thus no clear association between changes in the selected inflammatory gene transcripts or macrophage (subtype) counts and improvements in fibrosis, also in view of the finding that low-dose icosabutate was efficacious in reducing fibrosis.

There is no ideal rodent model, including the CD-diet model, that accurately reflects all components of human NASH (41). We chose the CD-diet model as it mirrors important phenotypical and mechanistic features of human NASH (22, 41). The CD-diet used in the current study is designed to induce inflammation and fibrosis by firstly preventing the hepatic export of lipids via a decrease in choline-dependent VLDL synthesis and secondly by depleting the liver of glutathione (GSH), a pivotal intracellular thiol limiting lipid peroxide- and free radical-induced damage (36). With respect to the first stressor, i.e., the accumulation of hepatic lipids, icosabutate ameliorated the CD-diet induced increases in both the abundant hepatic lipids (TAG, DAG and cholesteryl esters (CE)), and decreased the less abundant but highly bioactive arachidonic acid (AA) and linoleic acid (LA) derived oxylipins. AA-derived HETEs are believed to be involved in the pathogenesis of both human and murine NASH (8). However, the differences in hepatic HETEs between the CS- and CD-diet mice were not significant. Thus, although it is possible that reduction in hepatic HETEs has an ameliorative effect, they do not appear to play a pivotal role in driving the CD-diet induced liver pathology. On the contrary, the CD-diet induced a pronounced increase in hepatic 9,12,13-TriHOME (an oxidised linoleic acid metabolite) levels.

This finding suggests that free-radical (non-enzymatic) induced peroxidation is a more important driver of the liver pathology than enzymatic oxygenation.

This assumption also concurs with the significant decrease in hepatic GSH in response to the CD-diet, an effect exacerbated by EPA treatment. This likely reflects increased GSH utilization in EPA-fed mice in response to PUFA peroxidation. Given the beneficial effects of reversal of hepatic GSH deficiency on fibrogenesis (10, 42), the exacerbation of GSH depletion may underlie the worsening in liver fibrosis in response to EPA. Importantly, hepatic GSH and GSH/GSSG were unchanged in EPA-treated mice fed the CS-diet. This indicates that EPA is not a pro-oxidant *per se* - indeed studies have shown that LCn-3FAs can lower markers of oxidative stress (43). More likely, we suggest that conditions characterized by increased hepatic lipid peroxidation are unsuitable for therapeutic interventions with LC-PUFAs, as has been previously shown in both NASH and ASH (15, 16).

The ability of icosabutate to avoid worsening of the GSH depletion induced by EPA is likely related to its minimal incorporation into cellular membranes. Moreover, icosabutate improved the hepatic GSH/GSSG ratio. Reduced GSH requirements and formation of GSSG likely result from lower formation of lipid peroxides, e.g., the decrease in 9,12,13-TriHOME, seen in response to icosabutate therapy. To what extent decreased inflammation is driving the reductions in markers of hepatic oxidative stress, or vice versa, is uncertain. Interestingly the arachidonic acid cascade, which is downregulated by icosabutate, is a major source of cellular reactive oxygen species (44).

In addition, avoidance of cellular storage and β-oxidation may allow icosabutate to achieve the extracellular concentrations required for activation of the LCn-3FA receptor, FFAR4. Indeed, we demonstrate that icosabutate is a full FFAR4 agonist, engaging the β-arrestin-2 pathway with an EC50 that is 3-fold lower than the portal vein C_{max} in rats given a therapeutic dose (19). FFAR4 is highly expressed on macrophages/Kupffer cells (6), and its activation with high-dose LCn-3FA feeding in mice has potent anti-inflammatory effects that in turn improve glycemic control (6). The prominent portal vein transport of icosabutate (19) likely further enhances the ability of icosabutate to achieve the hepatic concentrations required for targeting FFAR4 .

In the post-hoc analysis of plasma samples from earlier clinical trials in subjects at increased risk of NASH and CVD (hyperlipidemic, overweight/obese), the rapid and marked decrease in both plasma ALT and AST (markers of liver inflammation and hepatocyte stress) and GGT (a marker of cellular glutathione metabolism/oxidative stress) in response to icosabutate provides evidence that the findings observed in our rodent studies appear to translate to humans. As decreases in ALT (>17 U/L) are associated with histological responses to therapy in patients with NASH (45), the 29 U/L (49%) decrease in median ALT observed in our clinical studies is promising, especially as significant improvements were observed at all time-points. The clinical relevance of the marked reductions in liver enzymes is further supported by the significant decrease in FIB-4 in subjects with elevated baseline ALT and/or AST. An increase in FIB-4 over time is associated with an increased risk of severe liver disease whilst a decrease is associated with a lower risk (34). Our finding that 4 of 7 subjects treated with icosabutate dropped from FIB-4 levels associated with 'intermediate' to 'low' risk (34) is therefore encouraging. The on-going phase 2 ICONA study (NCT04052516) will specifically address the efficacy of once-daily oral icosabutate (300 mg or 600 mg) for 52 weeks compared with placebo in patients with NASH with biopsy follow-up. In relation to doses used in the current study in mice, the ICOSA-L dose equates to approximately 318 mg/day in humans whereas ICOSA-H corresponds to 636 mg/day using interspecies allometric scaling (46).

In summary, the current studies demonstrate that, unlike EPA, icosabutate avoids hepatocyte accumulation *in vitro*. In a delayed treatment CD-diet rodent NASH model, icosabutate prevented the CD-diet-induced increases in NASH associated lipids and induced a potent anti-fibrotic effect. In contrast, EPA accumulated in hepatocytes *in vitro* and amplified the hepatic GSH depleting effects of the CD-diet and promoted fibrosis. The translatability of the pre-clinical findings is supported by clinical data where icosabutate rapidly improved multiple markers of liver injury in patients at risk of NASH. Esterification resistant LCn-3FAs, as exemplified here by icosabutate, may thus offer a novel and efficacious therapeutic approach for the treatment of fibrosing NASH.

References

1. Musso G, Cassader M, Paschetta E, Gambino R. Bioactive Lipid Species and Metabolic Pathways in Progression and Resolution of Nonalcoholic Steatohepatitis. Gastroenterology. 2018;155(2):282-302 e8.
2. Kazankov K, Jorgensen SMD, Thomsen KL, Moller HJ, Vilstrup H, George J, et al. The role of macrophages in nonalcoholic fatty liver disease and nonalcoholic steatohepatitis. Nat Rev Gastroenterol Hepatol. 2019;16(3):145-59.
3. Schuppan D, Surabattula R, Wang XY. Determinants of fibrosis progression and regression in NASH. J Hepatol. 2018;68(2):238-50.
4. Jakubowski JA, Ardlie NG. Evidence for the mechanism by which eicosapentaenoic acid inhibits human platelet aggregation and secretion - implications for the prevention of vascular disease. Thromb Res. 1979;16(1-2):205-17.
5. Han YH, Shin KO, Kim JY, Khadka DB, Kim HJ, Lee YM, et al. A maresin 1/RORalpha/12-lipoxygenase autoregulatory circuit prevents inflammation and progression of nonalcoholic steatohepatitis. J Clin Invest. 2019;130:1684-98.
6. Oh DY, Talukdar S, Bae EJ, Imamura T, Morinaga H, Fan W, et al. GPR120 is an omega-3 fatty acid receptor mediating potent anti-inflammatory and insulin-sensitizing effects. Cell. 2010;142(5):687-98.
7. Loomba R, Quehenberger O, Armando A, Dennis EA. Polyunsaturated fatty acid metabolites as novel lipidomic biomarkers for noninvasive diagnosis of nonalcoholic steatohepatitis. J Lipid Res. 2015;56(1):185-92.
8. Hall Z, Bond NJ, Ashmore T, Sanders F, Ament Z, Wang X, et al. Lipid zonation and phospholipid remodeling in nonalcoholic fatty liver disease. Hepatology. 2017;65(4):1165-80.
9. Sanyal AJ, Abdelmalek MF, Suzuki A, Cummings OW, Chojkier M, Group E-AS. No significant effects of ethyl-eicosapentanoic acid on histologic features of nonalcoholic steatohepatitis in a phase 2 trial. Gastroenterology. 2014;147(2):377-84 e1.
10. Mohs A, Otto T, Schneider KM, Peltzer M, Boekschoten M, Holland CH, et al. Hepatocyte-specific NRF2 activation controls fibrogenesis and carcinogenesis in steatohepatitis. Journal of Hepatology.
11. Berbee JFP, Mol IM, Milne GL, Pollock E, Hoeke G, Lutjohann D, et al. Deuterium-reinforced polyunsaturated fatty acids protect against atherosclerosis by lowering lipid peroxidation and hypercholesterolemia. Atherosclerosis. 2017;264:100-7.
12. Brown JE, Wahle KW. Effect of fish-oil and vitamin E supplementation on lipid peroxidation and whole-blood aggregation in man. Clin Chim Acta. 1990;193(3):147-56.
13. Brude IR, Drevon CA, Hjermann I, Seljeflot I, Lund-Katz S, Saarem K, et al. Peroxidation of LDL from combined-hyperlipidemic male smokers supplied with omega-3 fatty acids and antioxidants. Arterioscler Thromb Vasc Biol. 1997;17(11):2576-88.
14. Guichardant M, Calzada C, Bernoud-Hubac N, Lagarde M, Vericel E. Omega-3 polyunsaturated fatty acids and oxygenated metabolism in atherothrombosis. Biochim Biophys Acta. 2015;1851(4):485-95.
15. Depner CM, Traber MG, Bobe G, Kensicki E, Bohren KM, Milne G, et al. A metabolomic analysis of omega-3 fatty acid-mediated attenuation of western diet-induced nonalcoholic steatohepatitis in LDLR-/- mice. PLoS One. 2013;8(12):e83756.
16. Warner DR, Liu H, Ghosh Dastidar S, Warner JB, Prodhan MAI, Yin X, et al. Ethanol and unsaturated dietary fat induce unique patterns of hepatic omega-6 and omega-3 PUFA oxylipins in a mouse model of alcoholic liver disease. PLoS One. 2018;13(9):e0204119.
17. Song JH, Miyazawa T. Enhanced level of n-3 fatty acid in membrane phospholipids induces lipid peroxidation in rats fed dietary docosahexaenoic acid oil. Atherosclerosis. 2001;155(1):9-18.

18. Schuchardt JP, Hahn A. Bioavailability of long-chain omega-3 fatty acids. Prostaglandins Leukot Essent Fatty Acids. 2013;89(1):1-8.
19. van den Hoek AM, Pieterman EJ, van der Hoorn JW, Iruarrizaga-Lejarreta M, Alonso C, Verschuren L, et al. Icosabutate Exerts Beneficial Effects Upon Insulin Sensitivity, Hepatic Inflammation, Lipotoxicity, and Fibrosis in Mice. Hepatol Commun. 2020;4(2):193-207.
20. Stokman G, van den Hoek AM, Denker Thorbekk D, Pieterman EJ, Skovgard Veidal S, Basta B, et al. Dual targeting of hepatic fibrosis and atherogenesis by icosabutate, an engineered eicosapentaenoic acid derivative. Liver Int. 2020;40(11):2860-76.
21. Matsumoto M, Hada N, Sakamaki Y, Uno A, Shiga T, Tanaka C, et al. An improved mouse model that rapidly develops fibrosis in non-alcoholic steatohepatitis. Int J Exp Pathol. 2013;94(2):93-103.
22. Wei G, An P, Vaid KA, Nasser I, Huang P, Tan L, et al. Comparison of murine steatohepatitis models identifies a dietary intervention with robust fibrosis, ductular reaction, and rapid progression to cirrhosis and cancer. Am J Physiol Gastrointest Liver Physiol. 2020;318(1):G174-G88.
23. Kastelein JJ, Hallen J, Vige R, Fraser DA, Zhou R, Hustvedt SO, et al. Icosabutate, a Structurally Engineered Fatty Acid, Improves the Cardiovascular Risk Profile in Statin-Treated Patients with Residual Hypertriglyceridemia. Cardiology. 2016;135(1):3-12.
24. Bays HE, Hallen J, Vige R, Fraser D, Zhou R, Hustvedt SO, et al. Icosabutate for the treatment of very high triglycerides: A placebo-controlled, randomized, double-blind, 12-week clinical trial. J Clin Lipidol. 2016;10(1):181-91 e1-2.
25. Qin Y, Hallén J, Skjæret T, Odden E, Fraser D, Nyheim H, et al. Abstract 11889: Phase Ib Study of Icosabutate, a Novel Structurally Enhanced Fatty Acid, in Subjects With Hypercholesterolemia. Circulation. 2014;130(suppl_2):A11889-A.
26. Gaster M, Rustan AC, Aas V, Beck-Nielsen H. Reduced lipid oxidation in skeletal muscle from type 2 diabetic subjects may be of genetic origin: evidence from cultured myotubes. Diabetes. 2004;53(3):542-8.
27. Wensaas AJ, Rustan AC, Lovstedt K, Kull B, Wikstrom S, Drevon CA, et al. Cell-based multiwell assays for the detection of substrate accumulation and oxidation. J Lipid Res. 2007;48(4):961-7.
28. Bradford MM. A rapid and sensitive method for the quantitation of microgram quantities of protein utilizing the principle of protein-dye binding. Anal Biochem. 1976;72:248-54.
29. Ding X, Saxena NK, Lin S, Gupta NA, Anania FA. Exendin-4, a glucagon-like protein-1 (GLP-1) receptor agonist, reverses hepatic steatosis in ob/ob mice. Hepatology. 2006;43(1):173-81.
30. Wang X, Hausding M, Weng SY, Kim YO, Steven S, Klein T, et al. Gliptins Suppress Inflammatory Macrophage Activation to Mitigate Inflammation, Fibrosis, Oxidative Stress, and Vascular Dysfunction in Models of Nonalcoholic Steatohepatitis and Liver Fibrosis. Antioxid Redox Signal. 2018;28(2):87-109.
31. Ikenaga N, Peng ZW, Vaid KA, Liu SB, Yoshida S, Sverdlov DY, et al. Selective targeting of lysyl oxidase-like 2 (LOXL2) suppresses hepatic fibrosis progression and accelerates its reversal. Gut. 2017;66(9):1697-708.
32. Ashfaq-Khan M, Aslam M, Qureshi MA, Senkowski MS, Yen-Weng S, Strand S, et al. Dietary wheat amylase trypsin inhibitors promote features of murine non-alcoholic fatty liver disease. Sci Rep. 2019;9(1):17463.
33. Weng SY, Wang X, Vijayan S, Tang Y, Kim YO, Padberg K, et al. IL-4 Receptor Alpha Signaling through Macrophages Differentially Regulates Liver Fibrosis Progression and Reversal. EBioMedicine. 2018;29:92-103.
34. Hagstrom H, Talback M, Andreasson A, Walldius G, Hammar N. Repeated FIB-4 measurements can help identify individuals at risk of severe liver disease. J Hepatol. 2020;73(5):1023-9.
35. Newsome PN, Buchholtz K, Cusi K, Linder M, Okanoue T, Ratziu V, et al. A Placebo-Controlled Trial of Subcutaneous Semaglutide in Nonalcoholic Steatohepatitis. N Engl J Med. 2020.
36. Ursini F, Maiorino M. Lipid peroxidation and ferroptosis: The role of GSH and GPx4. Free Radic Biol Med. 2020;152:175-85.

37. Feldstein AE, Lopez R, Tamimi TA, Yerian L, Chung YM, Berk M, et al. Mass spectrometric profiling of oxidized lipid products in human nonalcoholic fatty liver disease and nonalcoholic steatohepatitis. J Lipid Res. 2010;51(10):3046-54.
38. Karsdal MA, Detlefsen S, Daniels SJ, Nielsen MJ, Krag A, Schuppan D. Is the Total Amount as Important as Localization and Type of Collagen in Liver Fibrosis Attributable to Steatohepatitis? Hepatology. 2020;71(1):346-51.
39. Hart KM, Fabre T, Sciurba JC, Gieseck RL, 3rd, Borthwick LA, Vannella KM, et al. Type 2 immunity is protective in metabolic disease but exacerbates NAFLD collaboratively with TGF-beta. Sci Transl Med. 2017;9(396).
40. Pellicoro A, Ramachandran P, Iredale JP, Fallowfield JA. Liver fibrosis and repair: immune regulation of wound healing in a solid organ. Nat Rev Immunol. 2014;14(3):181-94.
41. Farrell G, Schattenberg JM, Leclercq I, Yeh MM, Goldin R, Teoh N, et al. Mouse Models of Nonalcoholic Steatohepatitis: Toward Optimization of Their Relevance to Human Nonalcoholic Steatohepatitis. Hepatology. 2019;69(5):2241-57.
42. Caballero F, Fernandez A, Matias N, Martinez L, Fucho R, Elena M, et al. Specific contribution of methionine and choline in nutritional nonalcoholic steatohepatitis: impact on mitochondrial S-adenosyl-L-methionine and glutathione. J Biol Chem. 2010;285(24):18528-36.
43. Innes JK, Calder PC. The Differential Effects of Eicosapentaenoic Acid and Docosahexaenoic Acid on Cardiometabolic Risk Factors: A Systematic Review. Int J Mol Sci. 2018;19(2).
44. Woo CH, Eom YW, Yoo MH, You HJ, Han HJ, Song WK, et al. Tumor necrosis factor-alpha generates reactive oxygen species via a cytosolic phospholipase A2-linked cascade. J Biol Chem. 2000;275(41):32357-62.
45. Loomba R, Sanyal AJ, Kowdley KV, Terrault N, Chalasani NP, Abdelmalek MF, et al. Factors Associated With Histologic Response in Adult Patients With Nonalcoholic Steatohepatitis. Gastroenterology. 2019;156(1):88-95 e5.
46. Nair AB, Jacob S. A simple practice guide for dose conversion between animals and human. J Basic Clin Pharm. 2016;7(2):27-31.

Legend to Table 1

Table 1. Fractional partitioning of icosabutate versus EPA into cellular lipids of primary human hepatocytes

Incorporation of EPA or icosabutate into complex lipids [phospholipids (PL), triacylglycerol (TAG), cholesteryl ester (CE)] or as free fatty acid (FFA) in primary human hepatocytes after 24 h incubation (values in nmol/mg cell protein). Results are shown as means of 3 experiments (each with 4 parallels) ± SEM. ***p<0.001, ****p<0.0001 versus EPA, by unpaired t-test.

Legends to Figures

Fig. 1. Structural differences between icosabutate and EPA with effects on extracellular accumulation and utilisation as an energy source in primary human hepatocytes.

(A) Structural differences between EPA and icosabutate. (B) extracellular accumulation of EPA or icosabutate in primary human hepatocytes after 24 h incubation (values in nmol/mg cell protein). (C) ^{14}C-CO_2 production after incubation of the cells with ^{14}C-EPA or ^{14}C-icosabutate for 24 h (values in nmol/mg cell protein). Results (B, C) are shown as means of 3 experiments (each with 4 parallels) ± SEM. ****p<0.0001 versus EPA, by unpaired t-test.

Fig 2. Effects of treatments upon body weight, food intake, liver weight, plasma ALT and glucose tolerance.

Effects of treatments on (A) body weight, (B) food intake, (C) liver weight (D) alanine aminotransferase (ALT) (E) aspartate transaminase (AST) and (F) glucose tolerance in CS-diet-fed mice. *p<0.05, **p<0.01, ***p<0.001, ****p<0.0001 versus untreated CD-diet (versus untreated CS diet for glucose tolerance), by one-way ANOVA (two-way for glucose tolerance). CD, choline-deficient; CS, choline-sufficient.

Fig 3. Effects of icosabutate, EXE or EPA treatment on liver fibrosis.

(A) Representative images of Sirius Red (SR) stained livers (Scale bars indicate 50 μm). (B) relative hepatic hydroxyproline (HYP) (C) total HYP content (D) collagen content as measured by SR morphometry. *p<0.05, **p<0.01, ***p<0.001, ****p<0.0001 versus untreated CD-diet, by one-way ANOVA. CD, choline-deficient; CS, choline-sufficient.

Fig. 4. Effects of icosabutate and EXE on liver inflammation.

(A) Representative images of CD68+ and YM1+ stained livers from CD treatment groups (scale bars indicate 50 μm) (B) hepatic CD68+ cell numbers (C) hepatic YM1+ cell numbers. ***p<0.001 versus untreated CD-diet, by one-way ANOVA. CD, choline-deficient.

Fig. 5. Effects of treatment on key hepatic genes regulating inflammation and fibrosis.

Hepatic transcript levels for (A) type 1 collagen alpha 1 (Col1A1) (B) platelet derived growth factor receptor beta (PDGFRβ) (C) PDGF-B (D) tissue inhibitor of metalloproteinase (TIMP1) (E) alpha-smooth muscle actin (αSMA) (F) transforming growth factor beta (TGFβ1) (G) interleukin-1 beta (IL-1β) and (H) tumour necrosis factor alpha TNF-α. *p<0.05, **p<0.01, ***p<0.001, ****p<0.0001 versus untreated CD-diet, by one-way ANOVA. CD, choline-deficient; CS, choline-sufficient.

Fig. 6. Icosabutate avoids the EPA associated exacerbation of the CD-diet induced decrease in hepatic reduced glutathione (GSH) and inhibits the arachidonic acid (AA) cascade.

Effects of treatments on (A) GSH (B) oxidised glutathione (GSSG) (C) GSH/GSSG ratio (D) GSH/GSSG ratio in CS-diet fed mice only. Hepatic (E) diacylglycerol (DAG)-AA stores (F) phospholipid (PL, phosphatidylcholine)-AA stores. (G) Ratio of oxygenated linoleic acid (LA, 13-HODE) to LA, (H) the ratio of oxygenated AA metabolites (HETEs) to AA and hepatic HETEs (I-J), 13-HODE (K) and 9,12,13-TriHOME (L). *p<0.05, **p<0.01, ***p<0.001, ****p<0.0001 versus untreated CD-diet, by one-way ANOVA. CD, choline-deficient; CS, choline-sufficient.

Fig. 7. Icosabutate prevents CD-diet induced changes in the hepatic lipidome.

Colour code represents the transformed ratio between means of the groups: green sections denote metabolites that were reduced (negative $\log_2$ fold-changes) and red sections denote

increased metabolites (positive log_2 fold-changes). Data are presented as mean ± SEM, *p<0.05, **p<0.01, ***p<0.001 versus untreated CD-diet, by unpaired t-test. CD, choline-deficient; CS, choline-sufficient; Aa, amino acids; BCAA, branched-chain amino acids; BA, bile acids; F, free; GC, glycine conjugated; TC, total conjugated; ChoE, cholesteryl esters; SFA, saturated fatty acids; UFA, unsaturated fatty acids, DiHOME, dihydroxyoctadecenoic acids, oxoODE, oxo-octadecadienoic acids; oxFA, oxidised fatty acids.

Fig. 8. Icosabutate rapidly decreases markers of liver injury in a study population at high risk of NAFLD/NASH and CVD.

(A) Baseline characteristics of subjects treated with 600mg q.d. or placebo for up to 12 weeks. Decreases in elevated baseline plasma ALT (B), GGT (D) and AST (F) in response to treatment with icosabutate or placebo (C, E and G respectively). Change in FIB-4 in response to icosabutate (H) or placebo (I). Horizontal lines for liver enzymes represent reference normal cut-off values as defined in the clinical study report: ALT (>40 U/L), GGT (>38 U/L for females, >51 U/L for males), AST (>34 U/L). *p<0.05, **p<0.01, ***p<0.001, ****p<0.0001 versus baseline, by one-way ANOVA (B-G) or Wilcoxon paired signed rank test (H-I).

	5 µM		**25 µM**	
Lipid distribution	EPA	Icosabutate	EPA	Icosabutate
FFA	0.30 ± 0.02	0.04 ± 0.003****	0.77 ± 0.09	0.26 ± 0.01***
TAG	9.22 ± 1.02	1.01 ± 0.28****	34.8 ± 3.69	3.1 ± 0.55****
PL	13.0 ± 0.83	0.12 ± 0.01****	26.6 ± 1.42	0.69 ± 0.09****
CE	0.09 ± 0.06	0.01 ± 0.001****	0.09 ± 0.01	0.03 ± 0.002****
Total cellular lipids	**22.7 ± 1.8**	**1.18 ± 0.29****	**62.3 ± 4.9**	**4.1 ± 0.52****

Table 1

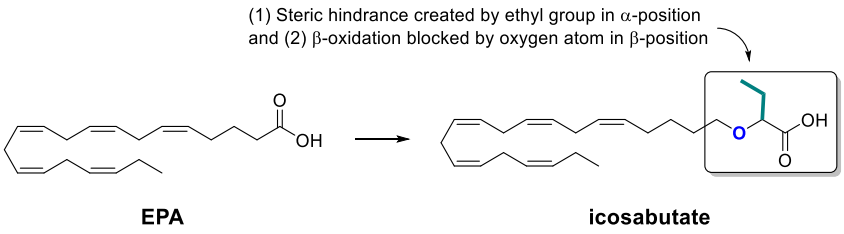

A

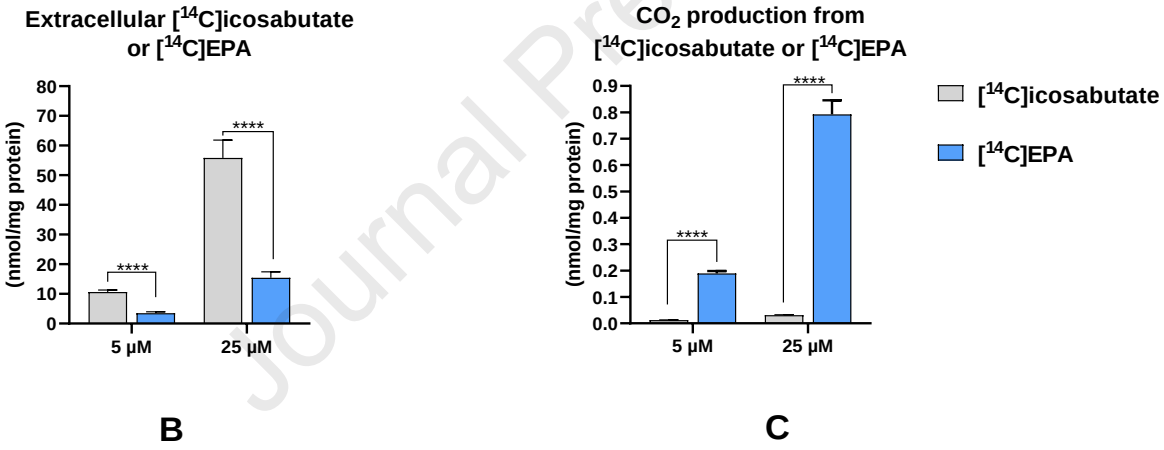

Fig.1

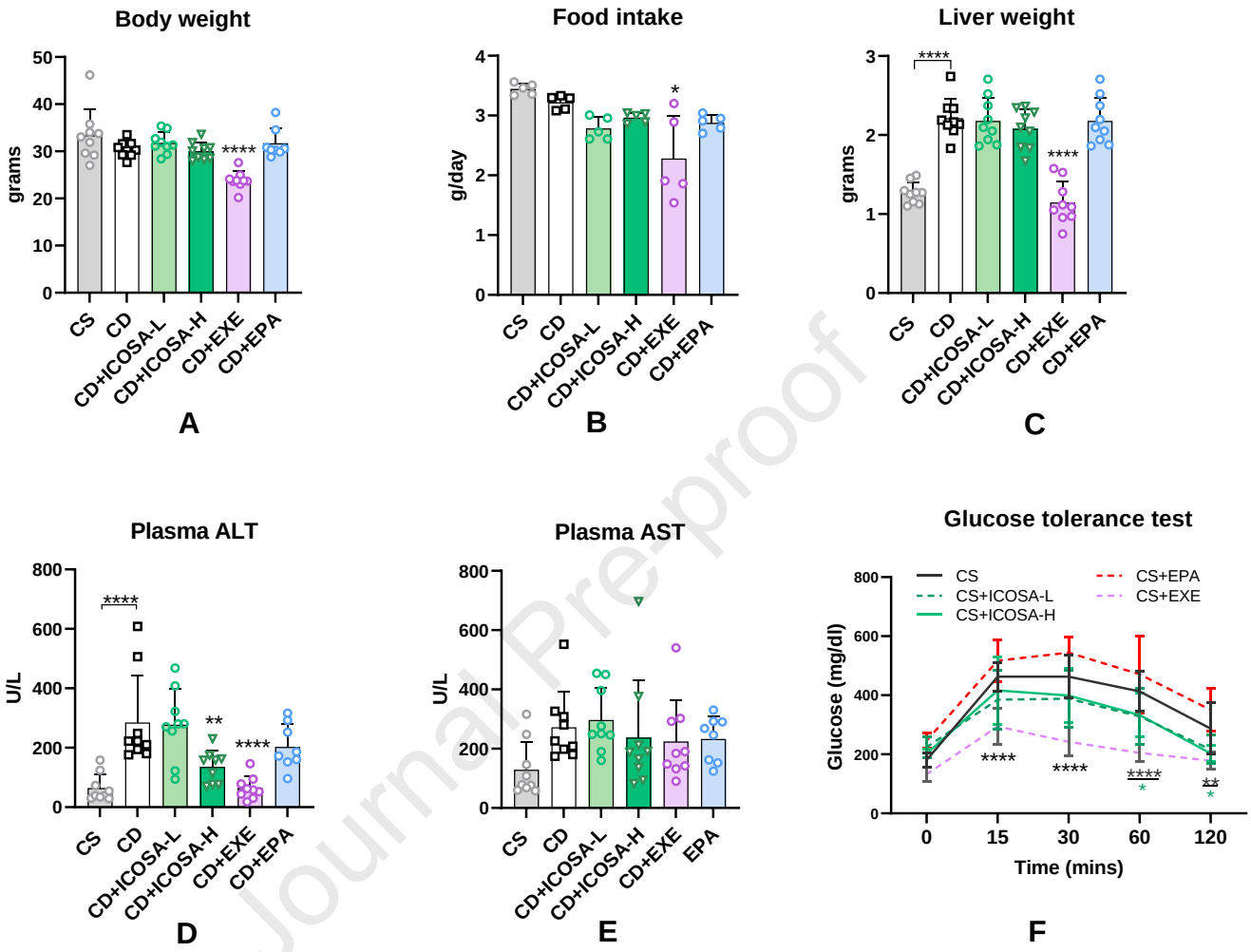

Fig. 2.

A

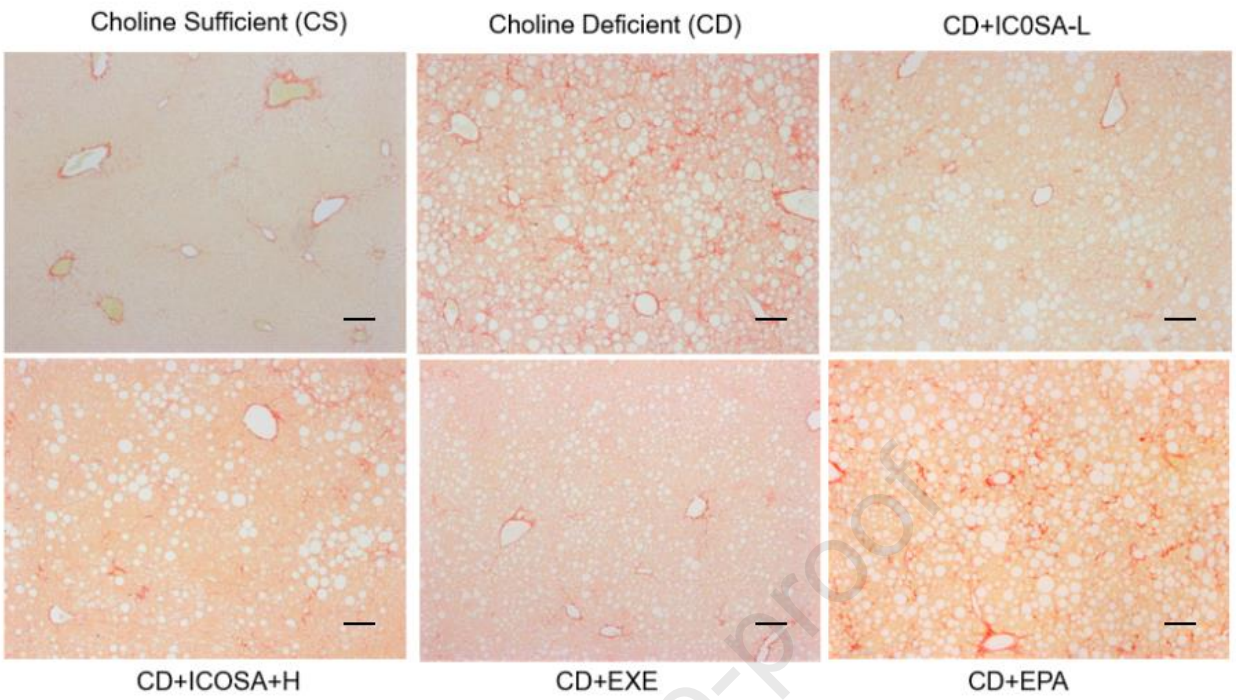

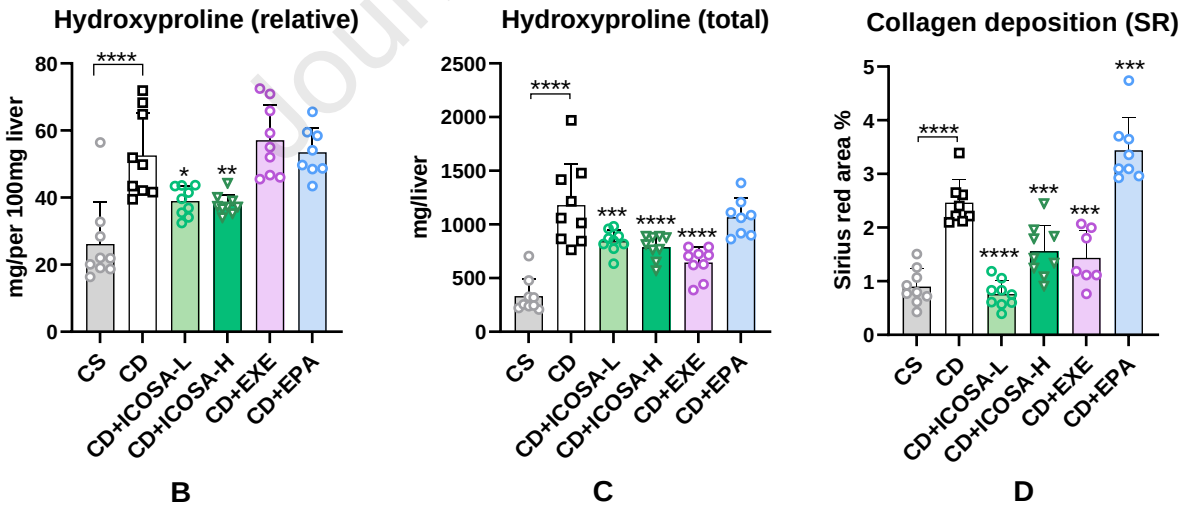

Fig. 3

A

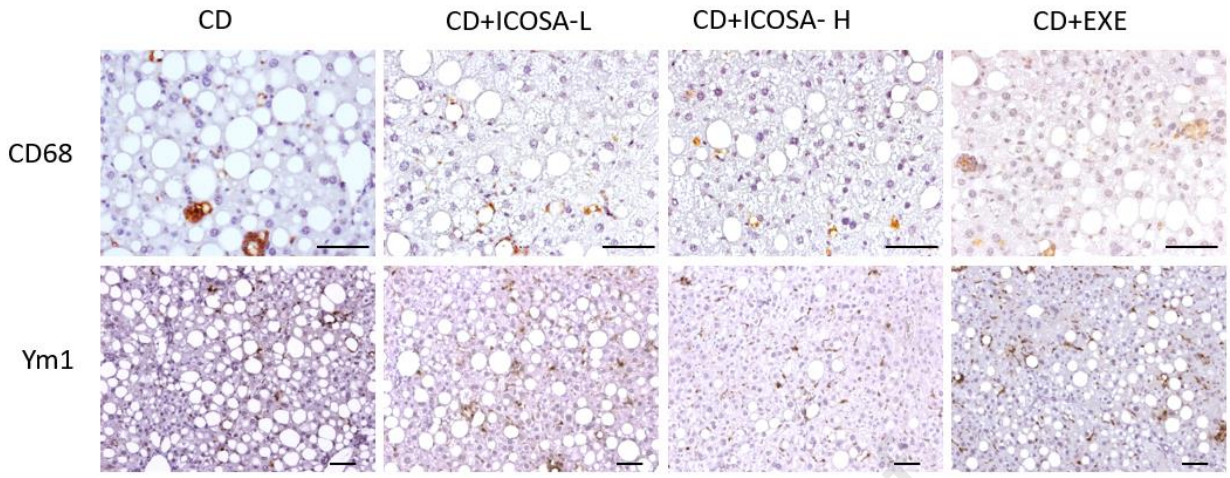

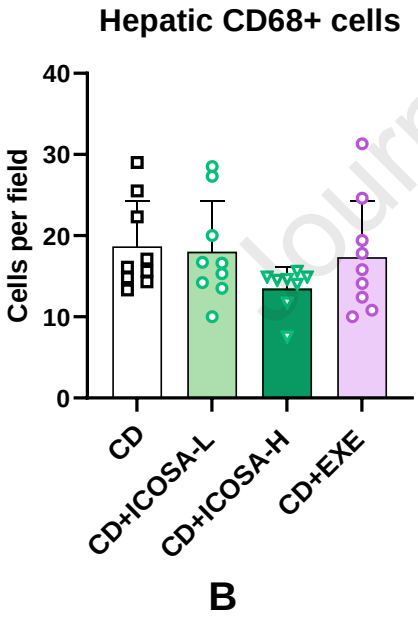

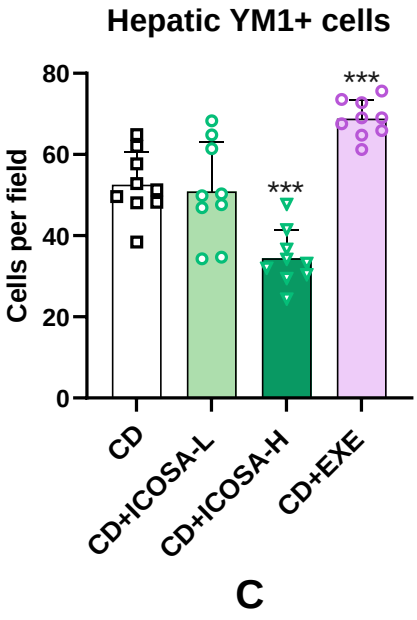

Fig. 4

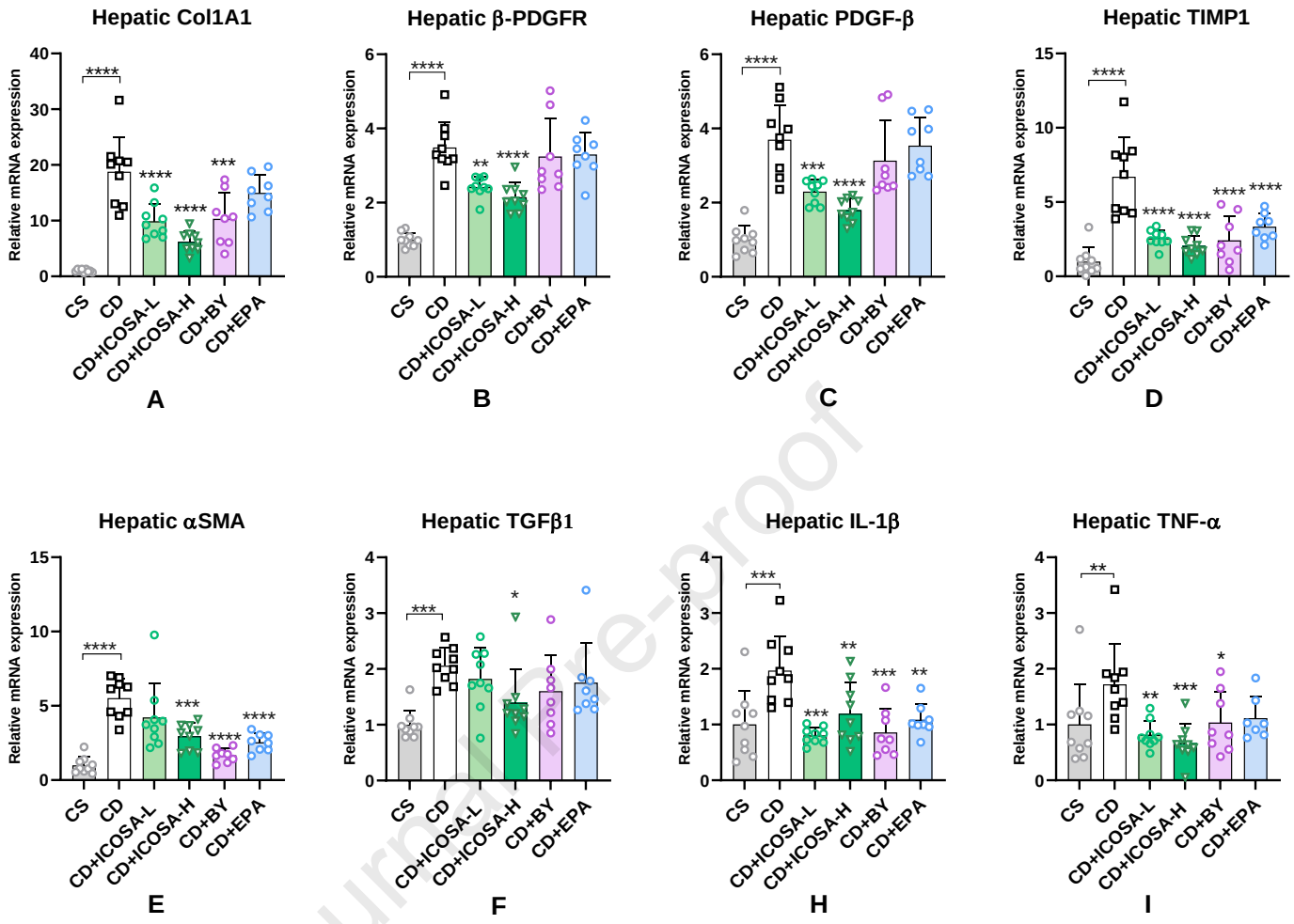

Fig. 5

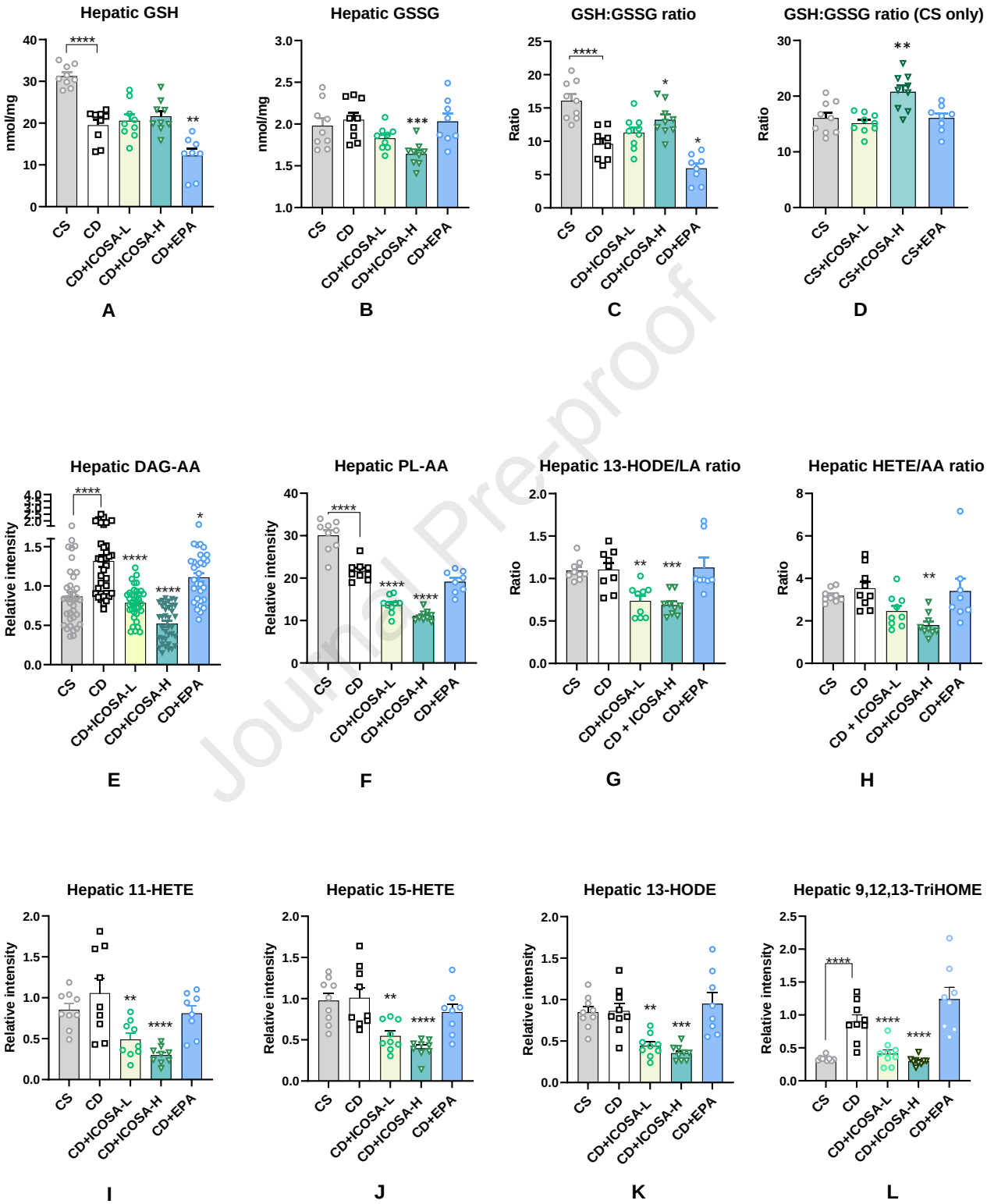
Hepatic GSH
nmol/mg
A
Hepatic GSSG
nmol/mg
B
GSH:GSSG ratio
Ratio
C
GSH:GSSG ratio (CS only)
Ratio
CS
CS+ICOSA-L
CS+ICOSA-H
CS+EPA
D
Hepatic DAG-AA
Relative intensity
E
Hepatic PL-AA
Relative intensity
F
Hepatic 13-HODE/LA ratio
Ratio
G
Hepatic HETE/AA ratio
Ratio
CD + ICOSA-L
H
Hepatic 11-HETE
Relative intensity
I
Hepatic 15-HETE
Relative intensity
J
Hepatic 13-HODE
Relative intensity
K
Hepatic 9,12,13-TriHOME
Relative intensity
L
CS
CD
CD+ICOSA-L
CD+ICOSA-H
CD+EPA

Fig. 6

Class	CD *vs*. CS		CD + EPA *vs*. CD		CD + ICOSA-L *vs*. CD		CD + ICOSA-H *vs*. CD	
	log_2 (fold-change)	Student´s *t*-test (*p*-value)	log_2 (fold-change)	Student´s *t*-test (*p*-value)	log_2 (fold-change)	Student´s *t*-test (*p*-value)	log_2 (fold-change)	Student´s *t*-test (*p*-value)
Amino acids								
Aa_and_Aa_derivatives	-0.27	2.72E-01	0.18	4.36E-01	0.43	3.91E-02	0.57	5.12E-02
BCAAs	-0.24	2.56E-01	0.26	2.62E-01	0.49	2.00E-02	0.63	2.52E-02
Sterol Lipids								
BA	0.33	2.66E-01	-0.63	2.70E-02	0.04	8.50E-01	0.24	4.23E-01
FBA	0.12	8.40E-01	-0.89	3.41E-02	-0.36	2.48E-01	0.45	3.41E-01
GCBA	1.23	1.24E-02	-1.00	4.56E-02	0.46	1.53E-01	0.31	4.38E-01
TCBA	0.23	3.51E-01	-0.42	7.86E-02	0.03	8.54E-01	0.09	7.02E-01
ChoE	1.57	9.95E-04	-0.23	4.77E-01	-0.32	3.75E-01	-1.19	2.97E-03
Fatty acids								
FA	0.18	8.86E-02	0.23	1.04E-02	-0.40	1.22E-03	-0.53	2.23E-05
FA.16.1	0.05	5.88E-01	0.10	3.91E-01	-0.22	4.68E-02	-0.15	2.17E-01
FA.18.1	0.16	3.49E-01	-0.004	9.78E-01	0.02	9.31E-01	-0.26	1.45E-01
FA.18.2	-0.01	9.76E-01	0.08	6.27E-01	-0.33	9.84E-02	-0.60	2.36E-03
FA.18.3	-0.07	7.95E-01	0.10	6.77E-01	-0.75	1.87E-02	-1.39	1.16E-03
FA_omega_3	0.01	9.79E-01	1.61	7.46E-08	-0.26	2.56E-01	-0.53	2.23E-02
FA_omega_6	0.37	1.85E-02	-0.17	2.60E-01	-0.80	1.67E-04	-1.11	1.61E-05
FA_omega_9	0.40	1.26E-01	-0.12	5.83E-01	0.04	8.69E-01	-0.28	2.35E-01
MUFA	0.07	4.59E-01	0.08	4.29E-01	-0.19	9.94E-02	-0.20	5.49E-02
PUFA	0.36	2.72E-02	0.34	1.45E-02	-0.62	1.06E-03	-0.90	7.63E-05
SFA	-0.11	6.92E-02	0.11	1.67E-02	-0.18	3.01E-04	-0.22	1.63E-04
UFA	0.25	4.08E-02	0.26	1.15E-02	-0.45	1.73E-03	-0.61	1.01E-04
Oxidized fatty acids								
HETE	0.29	2.84E-01	-0.11	7.77E-01	-0.83	2.45E-02	-1.45	2.27E-03
HODE	-0.32	1.54E-01	0.40	9.07E-02	-0.48	4.97E-02	-0.62	1.34E-02
DiHOME	-0.02	9.01E-01	0.31	1.80E-01	-0.42	3.88E-02	-0.52	7.60E-03
TriHOME	1.43	4.01E-04	0.46	1.09E-01	-1.14	5.49E-04	-1.59	2.32E-04
oxFA	-0.03	8.94E-01	0.20	3.74E-01	-0.51	3.35E-02	-0.75	2.75E-03
LAdoxFA	-0.17	3.69E-01	0.34	1.16E-01	-0.37	7.56E-02	-0.49	1.59E-02
oxoODE	-0.94	1.07E-02	-0.57	9.50E-02	0.90	2.87E-02	1.01	1.10E-03
Glycerolipids								
DAG	0.67	3.92E-06	-0.19	9.85E-02	-0.34	1.09E-03	-0.78	1.06E-06
TAG	0.80	1.41E-07	0.08	3.56E-01	-0.31	5.86E-04	-0.51	5.44E-06
Sat.TAG	0.31	7.51E-02	0.21	3.46E-01	-0.68	2.46E-03	-0.76	1.44E-03

Fig. 7

A

Baseline characteristics of the total study population

	Phase 1b: Hypercholesterolemia NCT02364635		Phase 2: Mixed dyslipidemia NCT01972178		Phase 2: Severe HTG NCT01893515	
	Icosabutate (n=18)	Placebo (n=6)	Icosabutate (n=56)	Placebo (n=57)	Icosabutate (n=43)	Placebo (n=44)
Age (mean)	56	51	58.7	58	53.5	51.6
BMI (mean)	28.1	27.3	31.5	31.7	31.7	32.3
Diabetes (%)	17	17	34	25	41.8	38.6
On statin (%)	100*	100*	100	100	20.5	20.9
Plasma TAG (mg/dl)	136**	192**	270	256	610	687
Non-HDL-C (mg/dl)	180**	205**	166	163	226	207

**All subjects were taken off statins 4-weeks prior to treatment with icosabutate for phase 1b*
***Lipid values are median except phase 1b (geometric mean)*

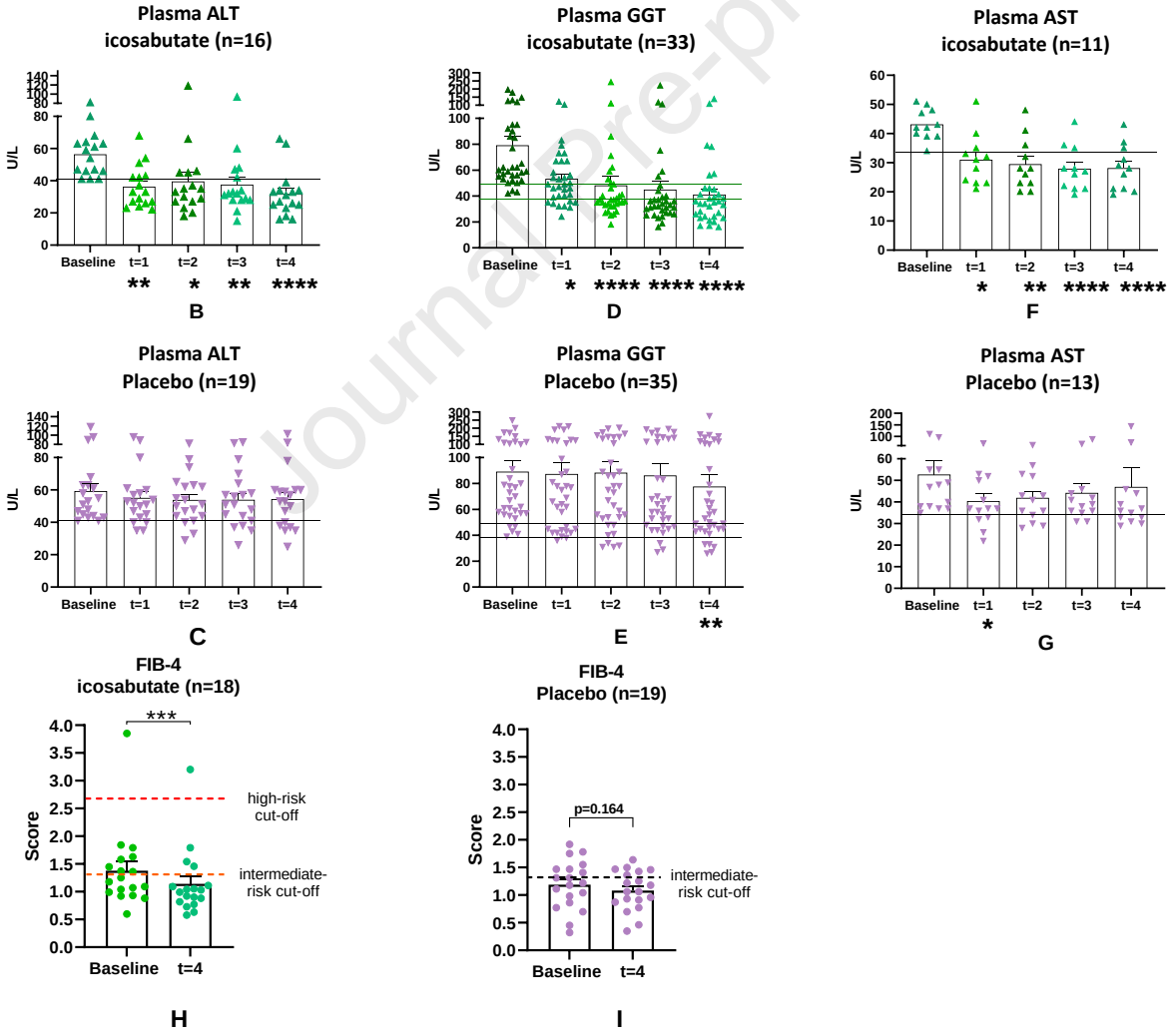

Fig.8

- The susceptibility of PUFAs to peroxidation may limit their efficacy in NASH
- Icosabutate, a modified PUFA derivative, has minimal incorporation into liver cells
- Icosabutate, but not EPA, reduces inflammation and fibrosis in mice
- Reduction in markers of liver injury after icosabutate treatment in humans
- Activation of FFAR4 (GPR120) may underlie the beneficial effects